Polymer Bulletin
https://doi.org/10.1007/s00289-019-03031-3

ORIGINAL PAPER

# Investigation of the gas permeability properties from polysulfone/polyethylene glycol composite membrane

**Danial Nasirian[1] · Iman Salahshoori[2] · Morteza Sadeghi[3] · Niloufar Rashidi[2] · Majid Hassanzadeganroudsari[2,4]**

Received: 3 April 2019 / Revised: 24 July 2019 / Accepted: 25 November 2019


## Abstract

In this research, the effect of polyethylene glycol (PEG) molecular weight on permeability and selectivity of polysulfone/polyethylene glycol (PSF/PEG) composite membrane is investigated. Polyethylene glycol with molecular weights of 4000, 6000, and 10,000 is applied. It is shown from the results that PEG applied in composite membranes with molecular weight of 1000 had the best diffusivity in comparison with the other composite membranes containing PEG with lower molecular weights. In addition, it is perceived that the permeability of $CO_2$ from PSF/PEG10000 composite membranes has increased with enhancing weight percent. $CO_2$ permeability into PSF/PEG composite membranes containing 20 wt% PEG10000 is calculated 7.64 barrer (1 barrer = $10^{-10}$ $cm^3$ (STP) cm/$cm^2$ s cmHg). The ideal selectivity for $CO_2/N_2$ gas pair in PSF pure membrane and composite membranes containing 10 wt% and 20 wt% PEG10000 are calculated 26.57, 30.61, and 32.12, respectively. Finally, the morphology and membrane structure of the membrane were evaluated with infrared spectroscopy (FTIR), X-ray diffraction (XRD), scanning electron microscopy (SEM), differential scanning calorimetry (DSC), thermogravimetric analysis (TGA), and tensile strength test.

**Keywords** Polysulfone · Polyethylene glycol · Composite membranes · Gas separation

✉ Majid Hassanzadeganroudsari
majid.hassanzadeganroudsari@vu.edu.au

[1] Department of Chemical Engineering, Shahreza Branch, Islamic Azad University, Isfahan, Iran

[2] Department of Chemical Engineering, Science and Research Branch, Islamic Azad University, Tehran, Iran

[3] Department of Chemical Engineering, Isfahan University of Technology, Isfahan, Iran

[4] Institute for Health and Sport, Victoria University, Melbourne, VIC, Australia

Published online: 29 November 2019

## Introduction

Recently, the polymeric membranes and their application on separation process have been studied to enhance the gas separation process efficiency [1]. Mixing polymers for manufacturing novel polymeric membranes is one of the efforts of researchers to increase the efficiency and modifying the characteristics of polymeric membranes in gas separation [2]. The process of polymer mixing with each other creates new properties, which are not found in one polymer, alone. Polymer–polymer interaction is able to not only affect the gas absorption and transport properties of the mixture but also impress their mechanical properties [3]. The main objective of most of the investigations in gas separation field is improvement in separation tendency from polymeric membranes [4]. It is worth noting that generally polymers are divided into glassy polymers and rubber polymers [5]. Rubber polymers are those which are soft in normal temperatures, and because of that in these materials, molecular absorption is more effective than their diffusion on permeability. However, in glassy polymers, which are hard and glassy in normal temperatures, diffusion is more effective on the permeability of these membranes [6]. Permeability (PA) and selectivity ($\alpha_{AB} = P_A/P_B$) are two prominent parameters in gas separation [7]. The modification of gases permeation and selectivity can be obtained by understanding the structure of the polymer and transport properties of membrane [8]. In recent decades, numerous investigations have been done to promote the efficiency of membrane using polyethers. Polyethylene glycol (PEG) is the most commonly applied polyethers due to having flexible main chain and great permeation of penetrants such as $CO_2$ and $CH_4$. However, due to weak mechanical and thermal resistance of PEG, it is utilization to make a thin layer can be faced with difficulties. Hence, based on the reports, in most of the composite membranes in which PEG is applied, PEG section improves permeability and selectivity and another section provides the ability of layer film forming with high chemical and thermal stability [9–12]. In this research, by adding PEG, the field for modifying the gas separation properties of the polysulfone membrane has been provided. The type of chains' development has an important role in diffusion properties from membrane due to morphology, crystallization, compression and glass transition temperature of membrane [13–15]. Finding structure and properties of polymeric membranes are key factors to obtain better efficiency of gas separation from membrane. Various investigations have been conducted on structures and properties of polysulfones [16, 17], polyimides [18–20], polycarbonates [21, 22], polyphenylene ethers [23, 24], poly(ether-block-amide)s [25–27], polyether ketones [28, 29], polydimethylsiloxane [30, 31], polyarylates [32, 33], poly(vinyl alcohol)s [34], and other polymers. Li et al. [12] studied polyethylene glycol (PEG) and cellulose acetate (CA) membranes. Permeability and selectivity of gas in some composite membranes were under investigation. They concluded that the addition of PEG20000 to CA causes a dramatic decrease in solubility into the membranes in temperature lower than 50 °C. Hence, the flexible main chain theory of PEG20000 in irregular areas of mixtures allows the big penetrants such as $CO_2$ and $CH_4$ to diffuse in the composite membranes easily. In

addition, it can be explained that the main cause of high diffusion coefficient of $CO_2$ compared with $N_2$ in high temperature is the high permeability of composite membranes for $CO_2$ compared with $N_2$. Kim et al. [35] investigated the diffusion of $CO_2$ through the filled pores of polyacrylonitrile (PAN) with polyethylene glycol (PEG). They investigated the composite membrane by FTIR, ESCA, and FE-SEM experiments and found out that polymer bond fills the pores of the bed. They considered that the high permselectivity of porous membrane with filled pores is due to high selective solubility of $CO_2$, which is implemented because of $CO_2$ tendency to PEO part. They used polyacrylonitrile (PAN) ultrafiltration membrane as bed and methoxypolyethylene glycol as filler. However, bed section helped the thermal and mechanical stability, and the existence of PEO section caused high selectivity of $CO_2/N_2$. Pore-filled composite membrane illustrated high efficiency for $CO_2/N_2$ separation. Chakrabarty et al. [36] investigated polysulfone and polyethylene glycol composite membranes with two different solvents. They used an asymmetric homogeneous solution with 12 wt% polysulfone, NMP (N-methyl-2-pyrrolidone), and DMAC (dimethyl acetamide) solvents and 5 wt% polyethylene glycol (PEG) containing three molecular weights (400, 6000, 20,000) as polymeric additive in casting solution for the preparation of polymeric membrane. Achieved membranes were evaluated using SEM and gas diffusivity experiment methods. They understood that regardless of solvent type, increase in the molecular weight of PEG from 400 to 20,000 eventuated in decreasing the average pore size of membrane although porosity and density of pores showed that gas permeability was increased dramatically. Sadeghi et al. [37] studied the effect of polyethylene glycol molecular weight on separation properties of PVC/PEG composite membrane. They used PEG with molecular weights of 400 to 4000. Composite membranes were fabricated applying thermal fuzzing inversion method from PVC/PEG/dimethylformamide solution at 60 °C, and permeability of $N_2$, $O_2$, $CH_4$ ,and $CO_2$ pure gases among fabricated membranes was measured at 25 °C and 20 bar. They observed that composite membrane with PEG4000 has the highest permeability for $CO_2$ and $CO_2/CH_4$ and $CO_2/N_2$ pair gases compared with the other composite membranes with lower PEG. In addition, they found out that in PVC/PEG4000 composite membrane, by increasing PEG weight percent, the amount of permeability increases. They found out that in this composite, due to soft section of polyethylene glycol and its good tendency to $CO_2$, the rate of permeability has increased, and due to the flexibility of PEG chains, permeability in composite membrane has increased. Yave et al. [38] by evaluating the gas permeability and free volume in poly (amide-b-ethylene oxide) and polyethylene glycol concluded that in overall free volume, it means by applying an appropriate softener (such as polyethylene glycol), which is effective on overall free surface and improvement in chain dynamism.

In this research, two prominent purposes were followed:

1. Improvement in gas separation properties from membrane by changing chemical composition of membrane

2. Improvement in gas separation properties from membrane by controlling membrane preparation conditions

The first purpose can be obtained by adding big electronegative or polar groups to macromolecules and the second target is possible by controlling the solvent extraction steps from solution. Among different membrane preparation methods, phase inversion technique was under the attention. This method can be applied for preparing polymeric membranes along with the other techniques, dry phase inversion, wet phase inversion, and thermal phase inversion [39]. Due to the matter that the properties of fabricated membrane by above-mentioned methods are different significantly, hence to prepare a membrane, the most appropriate membrane must be selected.

## Experiment

### Material

Polysulfone was purchased from (BASF-Germany), polyethylene glycol with molecular weights of 4000, 6000, and 10,000 was purchased from (Merck-Germany), and dimethylformamide as solvent was purchased from (Merck, Germany). In this research, $N_2$, $O_2$, $CH_4$ ,and $CO_2$ pure gases were applied for evaluating the experiments of membranes' permeability. $N_2$, $O_2$, and $CO_2$ gases with purity of 99.99% were purchased from Ardestan gas, Iran, and $CH_4$ with purity of 99.99% was bought by TGS company USA.

## Membrane preparation

Pure polysulfone membrane and composite membranes (polysulfone–polyethylene glycol) were prepared by thermal phase separation technique. Figure 1 shows chemical structures of PSF, PEG, and DMF respectively. Table 1 reveals chemical properties of PSF, PEG 4000, PEG 6000, PEG 10,000, and DMF. In this technique, polymer was dissolved in solvent at constant temperature and then is casted in casting mold. To fabricate membranes, at first, a 10 wt% polymeric solution made by dissolution of polymer in dimethylformamide solvent was under continuous stirring in a heat stirrer (C-mag HS 10 digital IKA, Germany) for 4 h at 60 °C for with the aim of preparing a homogeneous solution. Polymeric membrane was casted on clean glass plates and was put at 60 °C for 24 h to evaporate the solvent in normal oven. In order to complete evaporation of solvent in polymeric chains, prepared membranes were picked up from glass plates and were put in the vacuum oven (UV-12, Jeio-Tech, South Korea, and were dried during 4 h at 75 °C. Fabricated membranes had thickness between 40 to 60 μm. A micrometer measured the membranes' thickness. Figure 2 represents schematic preparation process of polymer membrane.

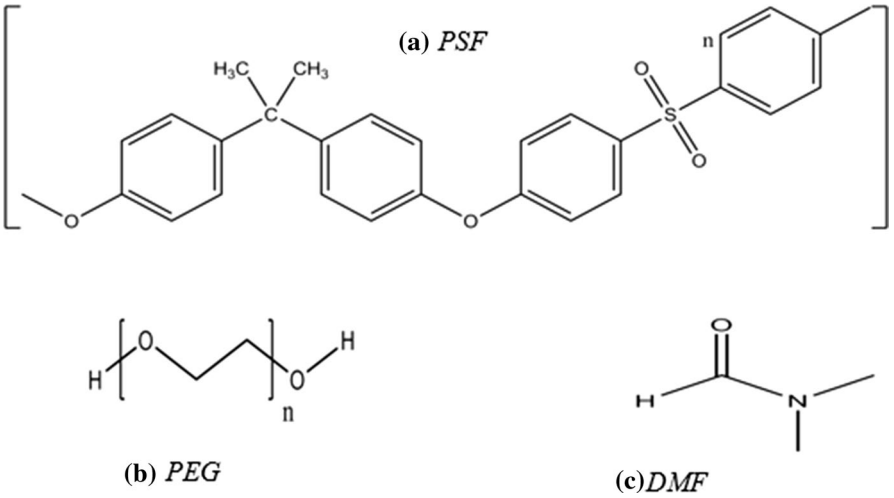


**Fig. 1** The schematic structure of the repeating unit for **a** PSF, **b** PEG, and **c** DMF

**Table 1** Physical properties of PSF, PEG 4000, PEG 6000, PEG 10,000, and DMF

| Sample | PSF | PEG 4000 | PEG 6000 | PEG 1000 | DMF |
|---|---|---|---|---|---|
| Molecular weight (g/mol) | 442.53 | 4000 | 6000 | 10,000 | 73.09 |
| Density (g/cm$^3$) | 1.24 | 1.2 | 1.2 | 1.2 | $9.49\times10^3$ |
| Solubility parameter (MPa)$^{1/2}$ | 20.26 | 20.2 | 20.2 | 20.2 | – |
| Glass temperature transition © | 185 | − 53–45 | − 53–45 | − 53–45 | – |
| Melting point © | 180–190 | 53–59 | 55–61 | 55–62 | – |

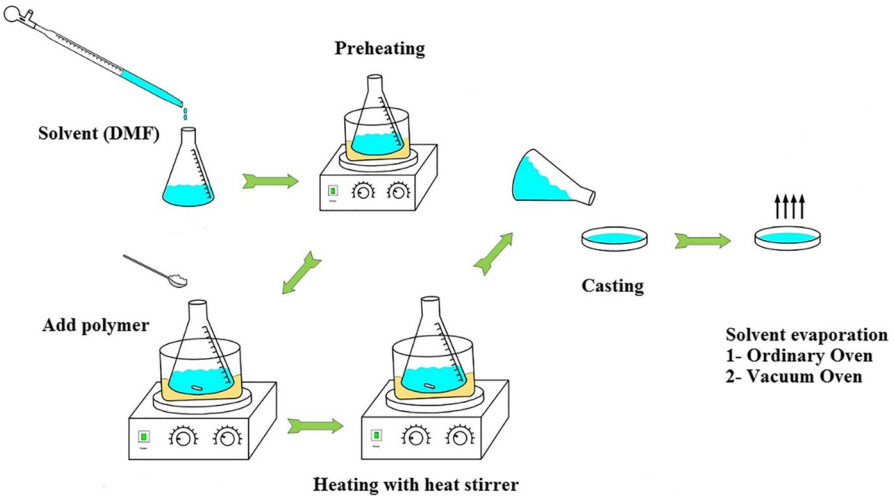


**Fig. 2** Schematic of the construction polymeric membranes process

## Membrane properties

### FTIR characterization

In order to recognize the bonds and chemical structure of samples, Fourier transform infrared spectroscopy (FTIR) test was applied. In this technique, light is brought into the surface of sample and the percentage of light passage or light absorption is measured by the spectrophotometer. Samples were placed in a spectrophotometer (Bruker Tensor 27, USA), and the spectra of each sample were obtained in the range of the wavenumbers 400 to 4000 $cm^{-1}$. Approximately, all compounds that have covalent bonding, whether organic or inorganic, absorb different frequencies of electromagnetic radiation in the infrared area. This method can be regarded a powerful and developed method for identifying functional groups and molecular structures. Due to the position of the peaks and their intensity, variety of bonds existed in the structure of the composition can be perceived.

## XRD analysis

The utilization of X-ray diffraction pattern (XRD) is one of the most basic methods for identifying and determining the purity of crystalline compounds. By this method of identification, beneficial information such as the presence of crystalline impurities, the presence of amorphous materials, and the effect of various processes in the change of the structure can be examined. The relative intensity and location of the peaks in the respective spectrum depend on the type and structure of the crystalline structure. In practice, this method is very appropriate for the identification of crystalline compounds. In order to identify the chemical composition and crystalline structure of the samples, X-ray diffraction spectroscopy (XRD) of the Philips X'pert Pro (Phillips, Netherlands) was applied. X-ray diffractograms with a diffraction angle ($\theta_2$) of 5° to 50° were recorded using copper irradiation under a voltage of 40 kV and a 40 mA amperage.

## SEM characterization

The morphology method of fabricated membranes by phase separation analysis was investigated using SEM (scanning electron microscope) (EM3200, KYKY). By using this method, it is possible to identify the morphology of surface, aggregation, shape, and average particle size. In addition, these images can be used to investigate and identify possible changes caused by morphology and particle shape and size after implementing some processes such as sample modification. The membrane samples were first broken up in transverse cross-section liquid nitrogen, and then an extremely thin layer of gold metal was coated on the surface of the case study to prevent the destruction of the cross-sectional structure in electron scanning. Covering

the membrane surface with gold is because non-conductive samples produce a good conductivity at their surface. The electron beam is emitted to the surface of the material and covers all of the sample points. In this way, a topographic image is obtained from the surface of the material.

## Tensile strength test

In this study, membrane was placed under a one-dimensional tensile force to investigate the tensile strength of tear. The tensile force was increased steadily during the test and the length change was recorded simultaneously (Zwick Z250, Germany). Samples (70 mm × 10 mm) were stretched at a constant speed of 5 $\frac{\text{mm}}{\text{min}}$. Temperature and stretching speed were constant. A sandpaper ($1 \times 1$ cm$^2$) was attached to the top and bottom of the sample to stabilize the membrane. Finally, applied force and strain (the ratio of the change in sample length to its initial length) was investigated. All results are expressed as a mean and three iterations ($n = 3$).

## Differential scanning calorimetry (DSC)

Differential scanning calorimetry (DSC) was used to determine the $T_g$ of the membranes. In addition, it was used to investigate the membrane miscibility or immiscibility of the composites. Moreover, the effect of nanoparticles on membrane has studied by DSC 8000 (Perkin Elmer). At the first step, a small portion of the sample was cut, and it was weighed. Then, this part was placed inside an aluminum enclosure. The samples were heated to 250 °C. The purpose of this step was eliminated the thermal history of the samples. Then, the sample was cooled to − 80 °C, and then again, it was heated to 250 °C. In the cooling step, $T_g$ membranes were measured. This test was performed in nitrogen atmosphere, and the heating rate was consistent at 10 °C/min.

## Thermogravimetric analysis (TGA)

Thermogravimetric analysis (TGA) is an analytical technique to determine the thermal stability and the fraction of volatile components. In this technique, mass change of sample is measured as a function of temperature. This analysis is also carried out under inert gas conditions such as He and $N_2$ and under oxide conditions in the presence of air. In this study, this method was used to investigate the effect of rubbery polymer (PEG) and glassy polymer (PSF) on the thermal stability of the prepared membranes. For this purpose, the TGA device manufactured by Mettler Toledo model (SDTA851e) was used. In this method, the prepared membranes and silica powder were heated from the ambient temperature to 700 °C and 900 °C in an atmosphere of nitrogen gas, and the heating rate was 10 °C/min.

## Membrane permeability

A constant pressure/variable volume system use nitrogen ($N_2$), oxygen ($O_2$), methane ($CH_4$), and carbon dioxide ($CO_2$) gases to evaluate the gas permeability test (Fig. 3). In constant pressure method, in order to measure the flow rate of gas passing through the membrane, the downstream volume should be discharged from the gas by connecting the downstream space to water column, and it is obtained by measuring the water column changes versus gas flow rate through the membrane. In this method, the changes of water column height versus time are plotted. By measuring the slope of the line in a steady-state condition and its multiplication in the cross section of the water column, the flow gas rate versus time will be obtained. Then the permeability of gas in membrane is calculated according to the following equation:

$$P = \frac{ql}{A\left(p_1 - p_2\right)}.$$

In this equation, $P$ is denoted as the permeability of gas which is expressed in barrer (1 barrer = $10^{-10}$ $cm^3$ (STP) cm/$cm^2$ s cmHg). $q$ is the flow rate of the permeated gas from the membrane per unit time ($cm^3$ (STP)/s), $l$ represents the average thickness of each membrane (cm), and $p_1$ and $p_2$ represent the absolute pressures in the feed area and permeated area, respectively (cmHg). A is the effective cross-sectional area of the membrane ($cm^2$). The ideal selectivity ($\alpha$ (A/B) can be calculated from the pure gas permeability ratio of components A and B based on the following equation:

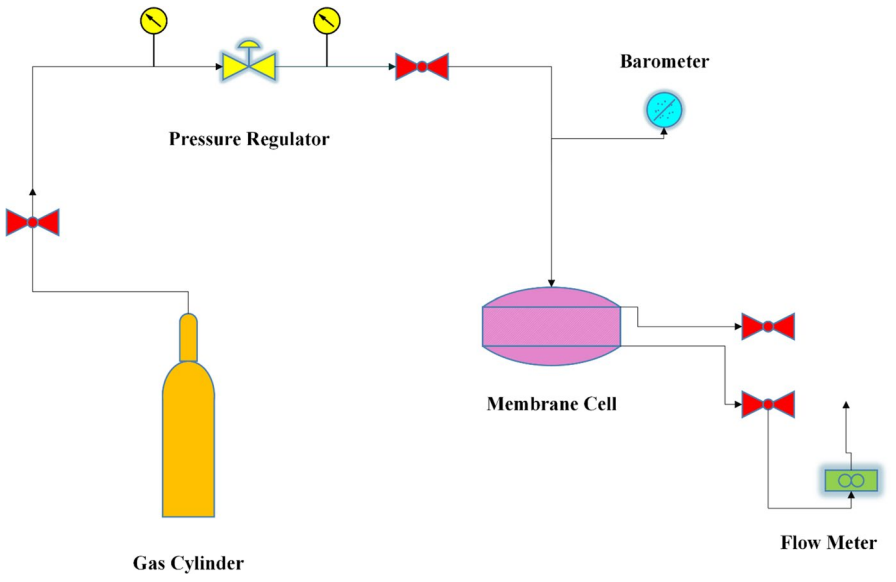


**Fig. 3** Schematic diagram of the experimental setup

$$\alpha_{A/B} = \frac{P_A}{P_B}$$

## Result and discussion

In this section, the characteristics of the pure membrane of polysulfone and the effect of increasing the polyethylene glycol with different molecular weights were investigated using FTIR, XRD, SEM, DSC, TGA, and tensile strength analysis tests. Then, the properties of gas permeability and selectivity were evaluated applying composite and pure membranes. To facilitate the analysis, membranes are named according to Table 2.

## FTIR spectra analysis

An FTIR test was applied to assess the manufacturing steps of polysulfone and polyethylene glycol in membrane preparation. Using this method and analyzing the obtained spectra, the chemical bonds formed in the material structure were identified and studied. The FTIR spectrum of pure PSF membrane and PSF/PEG composite membranes is shown in Fig. 4. Two strong absorptions observed at the wavelengths of 1494 $cm^{-1}$ and 1586 $cm^{-1}$ indicate an aromatic vibrational bonding of C=C in the polysulfone group. Strong absorption in 1146 $cm^{-1}$ shows the vibrational bonding of O=S=O in the structure of polysulfone. In addition, the strong absorption observed in wavelength of 1234 $cm^{-1}$ is related to the vibrational bonding of C–O–C in the ether group. The wavelength of 3056 $cm^{-1}$ is associated with the vibrational bonding of =C–H in the aromatic ring of polysulfone, and the two strong absorption observed at the wavelengths of 1298 $cm^{-1}$ and 1316 $cm^{-1}$ indicates the vibrational region of the sulfone group. Comparing the spectrum of membranes with polysulfone pure membrane, the highest change is related to the C–H bond with a wavelength of 2866 $cm^{-1}$. This strong absorption is related to the existence of $CH_2$ in the polyethylene glycol structure. With increasing molecular weight and polyethylene glycol percentage, the absorption rate is increased due to the increase in $CH_2$ group, which is shown in Fig. 5. Significant changes were not

**Table 2** Abbreviated name composite membranes

| Sample | Poly(ethylene glycol) in PSF-PEG hybrid membranes |
|---|---|
| PSF | – |
| PSF-10P4 | (10 wt%) of PEG 4000 |
| PSF-10P6 | (10 wt%) of PEG 6000 |
| PSF-10P10 | (10 wt%) of PEG 10000 |
| PSF-20P10 | (20 wt%) of PEG 10000 |

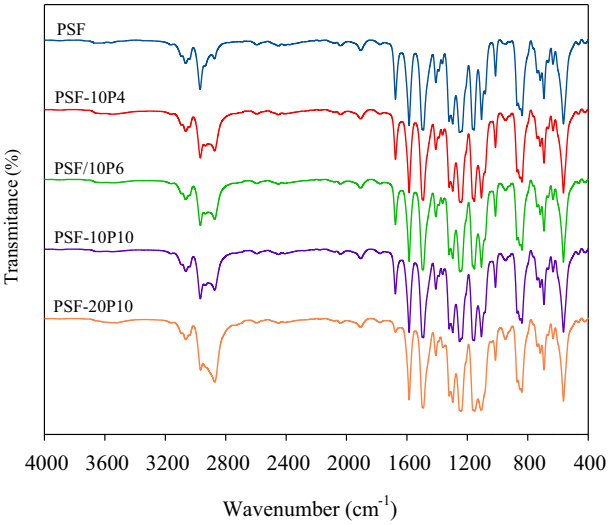


**Fig. 4** The FTIR spectra of PSF and PSF-PEG composite membranes

**Fig. 5** The FTIR spectra at C–H stretching region

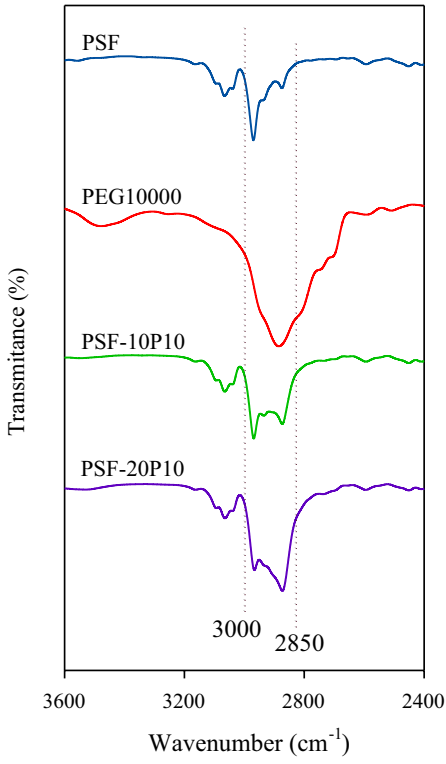

observed in the spectra, which is a sign of good compatibility and good interaction between these two polymers.

## XRD pattern analysis

Gas molecules are generally incapable of being spread in crystalline phases of the polymer. Therefore, the presence of crystalline domains in the polymer often leads to a decrease in gas permeability. X-ray diffraction pattern was used to investigate the possible crystallinity of PSF/PEG composite membranes. As shown in Fig. 6, all membranes made in this study are amorphous. Large peaks at high level of $\theta_2$ have been created due to poor molecular scattering, with amorphous empty spaces. The results showed that in all membranes there is a broad peak between 17.3° and 20°, which can be explained by the increase in PEG in mixed membranes. The XRD spectrum in high percentages of PEG indicated wide open spaces without crystals. As the PEG percentage increases, maximum peaks are shifted to ($\theta_2$) that is the average d-spacing of the PSF/PEG composite membranes, which increase with increase in PEG percentages. D-spacing change is increased in the amorphous region of the membrane. It also increases permeability. D-spacing is calculated by Bragg's law:

$$n\lambda = 2d \sin\theta,$$

where $n$ is the refractive index with integer values, $\lambda$ is the wavelength of the incident beam (Cu Kα, $\lambda = 0.15406$ nm), $2\theta$ is the diffraction angle between incident

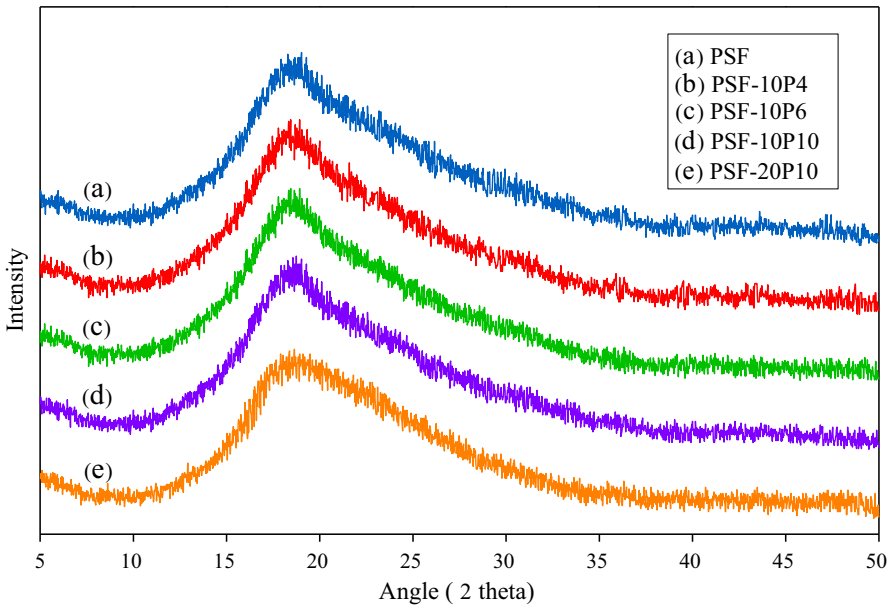


**Fig. 6** XRD patterns of the pure PSF and PSF-PEG composite membranes

and scattered X-ray wave vectors, and d is interlayer spacing of the lattice planes. According to Table 4, by increasing molecular weight of polyethylene glycol, the d-spacing increased that is entirely related to the gas permeability.

## SEM image analysis

Figure 7 illustrates the scanning electron microscope (SEM) images of the outer surface of the pure PSF membrane, and it is composite with polyethylene glycol. Polyethylene glycol in the PSF/PEG matrix is distributed in small regions and appears to be partially miscible. With increasing molecular weight and the amount of polyethylene glycol composition, the miscibility increases, and the mixing of two phases is such that it is difficult to detect two phases. Polysulfone was used as a phase modifier and bed for polyethylene glycol with different molecular weights due to its stability and chemical resistance. SEM images showed good distribution of polyethylene glycol in a polysulfone bed. The surface of the membrane has cavities that these cavities existed along the canals and carrier layers of pores in the membrane. The structure of the cavities has been modified due to the increase in the concentration of the polymer and, consequently, the reduction in solvent and non-solvent displacement velocity. Generally, the faster solvent and non-solvent displacement velocity in the coagulation stage, the greater probability of creating larger holes, and the slower velocity of solvent and non-solvent displacement in the coagulation system, the membrane structure tends to smaller cavities or ultimately cavity-free structures, which also change the structure, efficiency, flux, and flow of the membrane. In Fig. 8, the cross-sectional area of the membranes is shown. The dense structure of the membranes (which is more apparent in the membrane with 20% polyethylene glycol) results from the lack of observation of coarse holes, in which the structure can be distinguished by the proper distribution of the components. The cavities, which are visible in these images, are caused by the stresses in the casting stage and not the intrinsic porosity of the membrane. Microscopic scale can also be expected to have phase separation. The presence of transparent PEG masses in the structure of PSF network confirms this and shows that the two membrane-forming polymers, within the range of the desired composition, have a partial solubility. This fuzzy behavior corroborates the separation properties described for these membranes.

## Tensile strength analysis

The results of tensile strength of PSF membrane and composite membranes are summarized in Table 3. Providing an accurate prediction of strength behavior is challenging according to different parameters such as fragility of composites membrane [40]. Non-immiscible composite shows different mechanical properties compared to pure polymer [41, 42]. Regarding this, and by observing the results of Table 3, by adding polyethylene glycol with a weight of 4000 to the PSF polymer, we saw a decrease in the mechanical properties of the composite membranes, indicating a lack of complete membrane miscibility. However, by increasing the weight

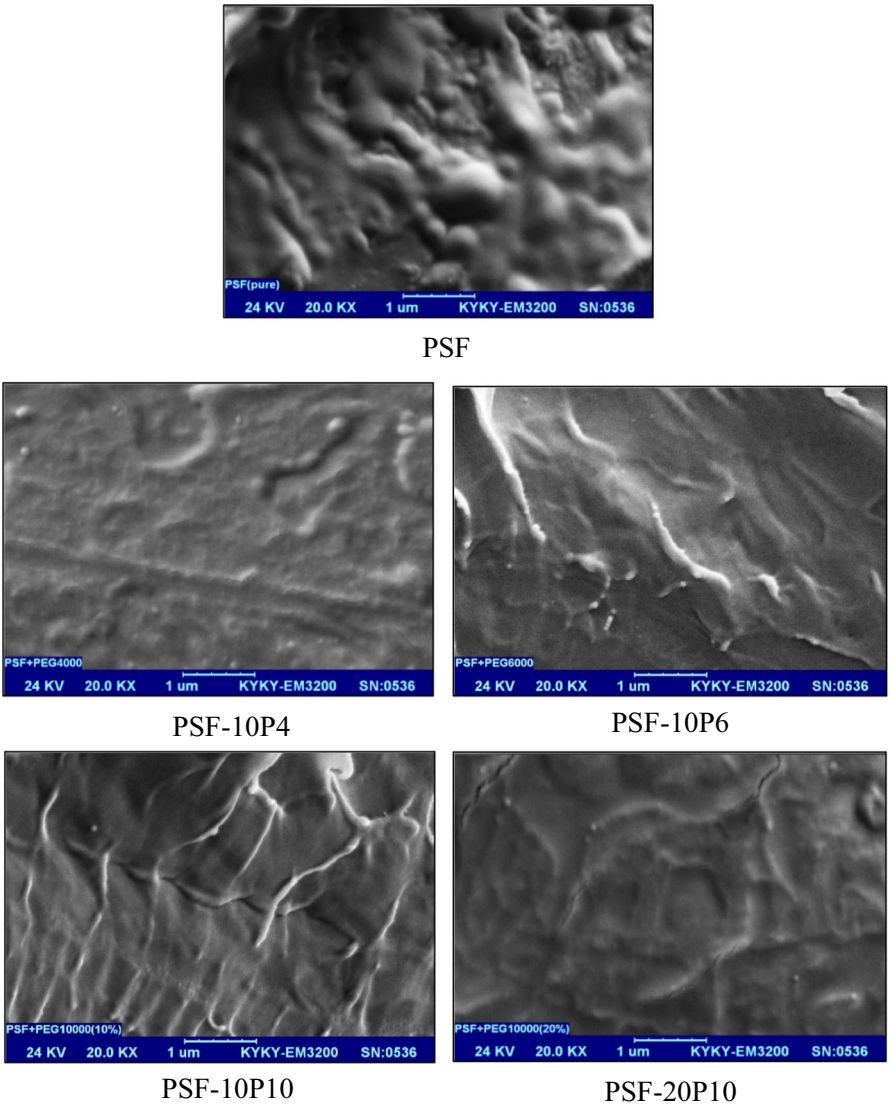


**Fig. 7** SEM photomicrographs of PSF and PSF-PEG composite membranes

percentage of PEG in the PSF, the mechanical properties of the composite membranes are increased compared to the pure PSF membrane, which indicates the high miscibility of these two polymers in high weight percentages of PEG. Polyethylene glycol is a rubbery polymer, which has a high mechanical strength and elasticity. Polyethylene glycol is a rubber polymer which has a high mechanical strength and elasticity [43]. Result reveals an increase in the Young's modulus, membrane's elasticity, and tensile strength that by mixing PEG on PSF membrane. With increasing molecular weight of PEG from 4000 to 6000, Young's modulus decreased, due

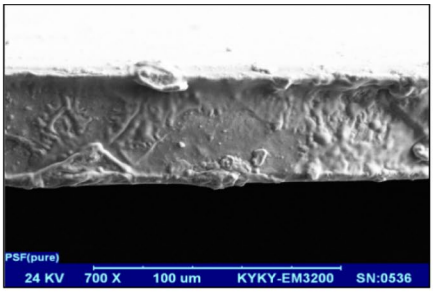


PSF

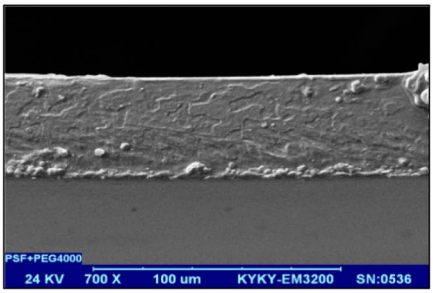


PSF-10P4

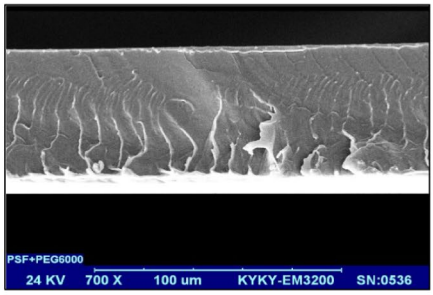


PSF-10P6

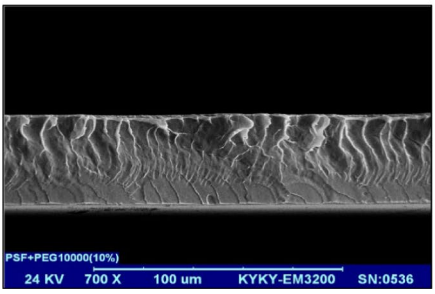


PSF-10P10

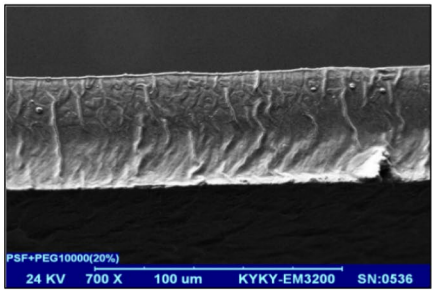


PSF-20P10

**Fig. 8** SEM photomicrographs of cross section of PSF and PSF-PEG composite membranes

**Table 3** D-spacing values (based on the XRD results) of the pure and composite membranes

| Sample | Position ($2\theta$°) | d-spacing (Å) |
|---|---|---|
| PSF | 20.2 | 2.11 |
| PSF-10P4 | 19.1 | 2.43 |
| PSF-10P6 | 18.6 | 2.98 |
| PSF-10P10 | 17.9 | 3.34 |
| PSF-20P10 | 17.1 | 3.87 |

to the immiscibility of polyethylene glycol in polymer in the PSF, resulting in less membrane tensile strength. However, with a molecular weight gain of polyethylene glycol, from 6000 to 10,000, Young's modulus increased due to the full miscibility of PEG in the PSF, which ultimately leads to an increase in the tensile strength of these membranes. By adding 10% PEG 4000 to 10% PEG 6000 to the pure PSF membrane, the tensile strength reached 63.1 MPa to 61.2 MPa, which indicates a reduction in tensile strength due to the immiscibility of two polymers. Also by adding 10% PEG 10,000 to 20% PEG 10,000 to the pure PSF membrane, the tensile strength reached 69.8 MPa to 79.4 MPa, and it illustrated uniform distribution of PEG 10,000 in the PSF, which is correlated with SEM result. Moreover, result shows that by augmenting concentration of PEG 10,000 from 10 to 20%, the Young's modulus increased from 2.31 GPa to 2.65 GPa, which indicated improvement in the elasticity of the composite membrane.

## DSC analysis

To determine the glass transition temperature (TG) of pure and composite membranes, the differential scanning calorimetry (DSC) with a weight percentage of 0, 4000, 6000, and 10,000 polyethylene glycol polymer was performed. Results are presented in Fig. 9. The DSC test provides valuable information on the hardness and flexibility of polymer chains [44, 45]. The results of the DSC test for pure polymers of PSF, PEG, and polymer composites PSF-10P4 and PSF-20P10 are presented in Fig. 9. As shown in Fig. 9, the glass transition temperature of the pure PSF and PEG were $T_g = 178.9$ °C and $T_g = -40.2$ °C, respectively. In addition, results revealed that there were two different $T_g$ in pure membrane for the PSF-10P4 membrane ($T_g = 28.3$ °C and $T_g = 133.1$ °C). Due to increase in density

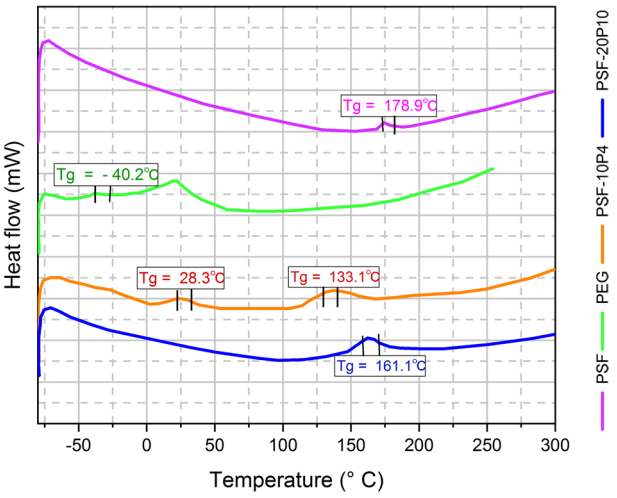


**Fig. 9** DSC test results of pure and composite membranes

of PEG, the miscibility increases. Therefore, two polymers achieved a single $T_g$ ($T_g = 161.1$ °C), which indicates the high miscibility of them. The DSC results in Fig. 9 represent correlation with SEM results (Fig. 7). Moreover, changing at the composite membranes surface area compared to pure membranes represents a decrease in crystalline grade of the composite membrane.

## TGA analysis

Figure 10 shows the TGA graphs for pure PSF, PEG membranes, and the PSF/PEG composite membranes. For PSF glassy polymer, the most weight loss is in the range of 500–700 °C, and for PEG rubbery polymer, more weight loss reported at the range of 400–600 °C. PSF glassy polymer showed higher thermal stability compared to PEG polymer. PSF-PEG composite encountered to two stages of thermal reduction. These two steps were related to the destruction of the polymeric chains of PSF and PEG. By adding PEG to the PSF matrix, it reduces thermal stability. However, by increasing the PEG weight percent in the PSF polymer, the overall weight loss reduced compared to the pure PSF membrane. However, increasing PEG weight percent caused an increase in thermal stability. Experiments were conducted at boiling point (DMF = 153C) to ensure that DMF was not present or present in samples. Total weight loss for pure and composite membranes was reported at 360 °C. Slight weight loss up to 360° indicates the membrane drying process. The sharp drop in the TGA isotherm starts at about 390° for all membranes, except for the PSF glassy membrane.

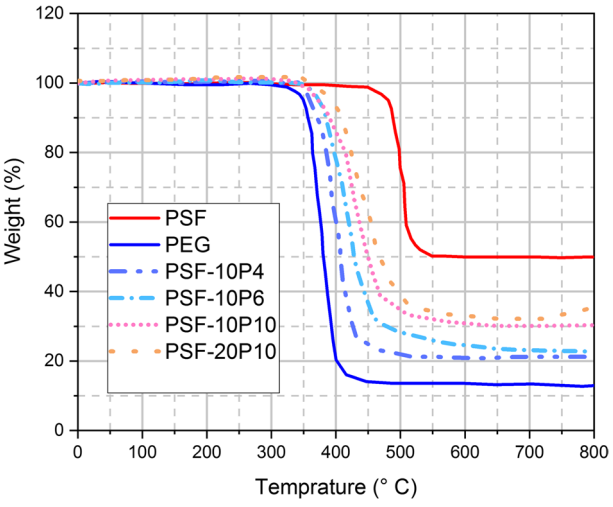


**Fig. 10** TGA curves of pure PSF, PEG, and composite membranes

**Table 4** Young's modulus and tensile strength of membranes

| Sample | Tensile strength (MPa) | Young's modulus (GPa) |
|---|---|---|
| PSF | 70.6 | 2.49 |
| PSF-10P4 | 63.1 | 2.04 |
| PSF-10P6 | 63.2 | 1.73 |
| PSF-10P10 | 69.8 | 2.31 |
| PSF-20P10 | 74.2 | 2.65 |

**Table 5** Permeability and selectivity of the gases in PSF and PSF-PEG hybrid membranes

| Membrane sample | Permeability (barrer) | | | | Selectivity | | |
|---|---|---|---|---|---|---|---|
| | $CO_2$ | $CH_4$ | $O_2$ | $N_2$ | $CO_2/CH_4$ | $CO_2/N_2$ | $O_2/N_2$ |
| PSF | 5.613 | 0.207 | 0.920 | 0.211 | 27.153 | 26.571 | 4.357 |
| PSF-10P4 | 5.644 | 0.218 | 1.063 | 0.218 | 25.875 | 25.875 | 4.875 |
| PSF-10P6 | 6.220 | 0.248 | 0.946 | 0.225 | 25.091 | 27.600 | 4.200 |
| PSF-10P10 | 7.115 | 0.255 | 1.190 | 0.232 | 27.889 | 30.610 | 5.122 |
| PSF-20P10 | 7.644 | 0.268 | 1.279 | 0.238 | 28.556 | 32.125 | 5.375 |

## Gas transport properties

The results of gas flow test within membranes are illustrated by a constant pressure system at 30 °C and 10 bar for $N_2$, $O_2$, $CH_4$, and $CO_2$ gases in Table 4. The kinetic diameter and condensation temperature of the investigated gases are presented in Table 3 [37]. As can be seen, the order of gas flow in the pure PSF membrane because of its existence as a glassy polymer is as follows:

$$CO_2 >> O_2 > N_2 > CH_4$$

$CO_2$ permeability differs greatly from the other investigated gases. This difference is due to high carbon dioxide condensation alongside a small kinetic diameter. Carbon dioxide has the property that causes membrane plasticization and polymeric chains to be opened. On the other hand, glassy polymers perform separation based on the size or kinetic diameter of gases. According to Table 5, the kinetic diameter of nitrogen is less than methane, so the nitrogen permeation should be higher than methane. On the other hand, methane has a higher condensation rate than nitrogen, and although in glass-based polymers separation is based on kinetic diameter, the condensability of the gas is not ineffective. Thus, the permeability of methane approaches the permeability of nitrogen in the pure Polysulfone membrane. By adding polyethylene glycol to the membrane structure and increasing the molecular weight as well as the composition of polyethylene glycol, the permeability of carbon dioxide increases in comparison with the other gases. The reasons for this increase are emitted in the form of elliptic

molecules of this gas which results in a lower kinetic diameter than other gases, polarization, and more condensation and also results in increasing the solubility coefficient [46]. Nitrogen, due to its nonpolar nature and neutrality, has low solubility in composite membranes. Therefore, its permeability is lower than the other gases. In addition, methane and oxygen have lower permeability compared with carbon dioxide, but their permeability becomes higher than nitrogen. This may be due to the smaller kinetic diameter of these gases compared with nitrogen [47]. By increasing polyethylene glycol, the permeability of methane becomes higher than nitrogen. This is due to the polyethylene glycol softening features that make the membrane properties closer to rubber membranes. In rubber polymers, the dominant mechanism is the dissolution process [37]. The determinant factor in the dissolution-penetration process is the amount of gas condensation. As a result, high condensability of, methane increases its viscosity in comparison with nitrogen. As can be observed, except membrane containing PEG 6000, the permeability of oxygen increases with increase in molecular weight of polyethylene glycol and its composition. Generally, the density of adhesion energy seems to increase with the increase in polar groups into a polymer [48]. The screening capability based on molecular size of PEG 6000 seems to be higher due to the semicrystalline nature of the other polymers studied here which results in poor conditions for molecular transfusion from the membrane. This behavior can be attributed to the hardening of the polymer chains and consequently, the screening capability by size. In other words, polar ether oxygen's in the PEG 6000 have more negative effect on the polymeric chain dynamic in comparison with the other studied polyethylene glycols. This is due to an increase in the density of adhesion energy that reduces the flexibility of the chain and thus reduces the permeability and selectivity of oxygen compared with nitrogen. Also in the composite membrane containing PEG 4000, due to the small increase in permeability of carbon dioxide, nitrogen, and methane in comparison with pure PSF membrane, the reduction in selectivity of carbon dioxide compared to nitrogen and methane can be seen. A composite membrane containing 20 wt% PEG10000 demonstrates a greater permeability than the other polyethylene glycol molecular weight. This is consistent with the finding that larger chains of polyethylene glycol make the $CO_2$ permeability more desirable [49]. In other words, polyethylene glycol with higher molecular weights will further increase the polar heads of the polymer in the composite membranes. This fact causes a clear tendency to increase the adsorption permeation coefficient, especially for carbon monoxide, which has instantaneous polarization. Regarding the permeability of gases, the maximum selectivity is for the pair gases of $CO_2/N_2$. These results can be attributed to the highest permeability of carbon dioxide gas and the lowest permeability of nitrogen gas for PSF/PEG composite membranes. In addition, in a composite membrane containing PEG 10,000 with a weight percent of 20%, it was observed that the selectivity of all pair gases increased compared with the pure PSF membrane. This is due to increased permeability of carbon dioxide due to increase of polar groups in polymeric composites. In Figs. 11 and 12, for the overall study of the effect of PEG increase in the composite membrane on degree of permeability and selectivity, the results are presented as a graph.

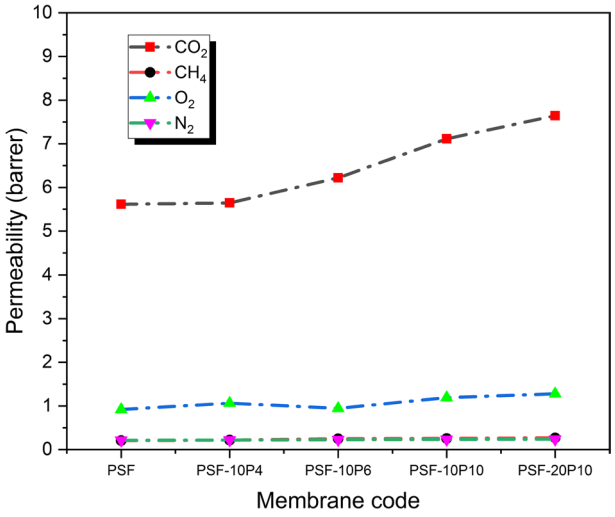


**Fig. 11** Single gas permeability of $CO_2$, $O_2$, $CH_4$ and $N_2$ in a PSF and PSF-PEG composite membranes

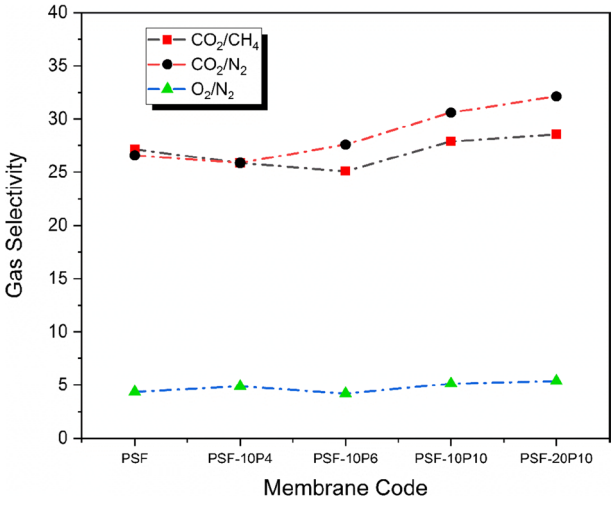


**Fig. 12** Ideal selectivity of $CO_2/N_2$, $CO_2/CH_4$, and $O_2/N_2$ in PSF and PSF-PEG composite membranes

## The effect of carbon dioxide gas and pressure on softening of membranes

$CO_2$ permeability data as a function of the pressure flowing through the membrane in a range of 2 to 10 bar for PSF pure membrane and its composite membranes are shown in Table 6. At pressures 2 to 10 bar, at first, the permeability decreases and begins to increase after reaching a critical pressure due to plasticization. By increasing pressure, the gas permeability is reduced, and this process continues until the

**Table 6** Condensability and Kinetic diameter of studied gases

| Gas component | Kinetic diameter (A°) | Condensability, critical temperature (K) |
|---|---|---|
| $CO_2$ | 3.3 | 304.2 |
| $O_2$ | 3.46 | 154.6 |
| $CH_4$ | 3.64 | 126.2 |
| $N_2$ | 3.8 | 190.6 |

polymer interacts with gas, and step by step with an increase in pressure, the permeability increases. This phenomenon is called softening or plasticization [50]. Plasticization by carbon dioxide can be occurred due to bipolar interactions between polymer polar groups and polarized carbon dioxide molecules [51]. As seen in Fig. 13, the permeability increases in less than 4 bar with decreasing pressure. Obviously, upstream gas pressure in higher pressure ranges does not have a significant effect on the permeation of carbon dioxide. Of course, in each case, the increase in permeability due to increased pressure can be because of increased absorption of carbon dioxide with bipolar moments in the membrane, which has a preferential affinity for this gas (especially approximately polyethylene glycol as an added polymer to the network). For highly absorbent gases such as carbon dioxide, high concentrations of gas at high pressures can increase the polymer's flexibility and, as a result, gas diffusion and ultimately permeation [48]. In addition, by increasing pressure, the increment of solubility of that gas which is more condensable ($CO_2$) increases the permeability coefficient [52]. Regarding the obtained values, it can be concluded that the addition of PEG10000 to the PSF grid, which has a high molecular weight, results in a more effective chain linkage (Table 7).

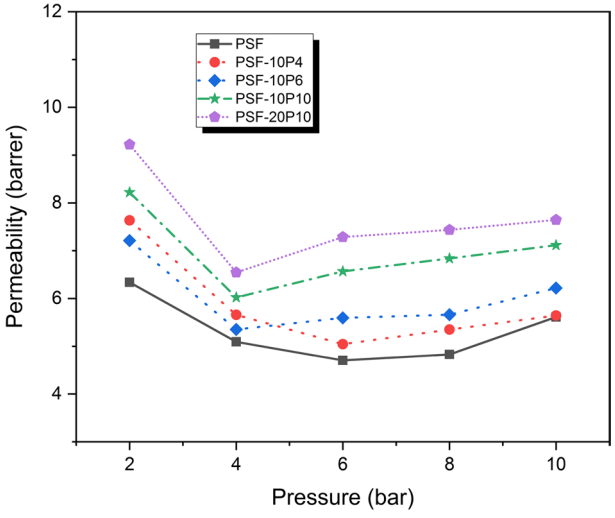


**Fig. 13** Effect of pressure on permeability of $CO_2$ in PSF and PSF-PEG composite membranes

**Table 7** The changes of permeation $CO_2$ with regards to the pressure passing through the membranes

| Membrane sample | Permeability $CO_2$ at various pressures based on (barrer) | | | | |
|---|---|---|---|---|---|
| | 2 bar | 4 bar | 6 bar | 8 bar | 10 bar |
| PSF | 6.338 | 5.093 | 4.703 | 4.829 | 5.613 |
| PSF-10P4 | 7.634 | 5.658 | 5.044 | 5.351 | 5.644 |
| PSF-10P6 | 7.211 | 5.352 | 5.596 | 5.662 | 6.220 |
| PSF-10P10 | 8.220 | 6.023 | 6.567 | 6.838 | 7.115 |
| PSF-20P10 | 9.221 | 6.544 | 7.287 | 7.436 | 7.644 |

## Conclusion

In this study, different weights of polyethylene glycol are added to the PSF grid to provide PSF/PEG composite membrane. In terms of membrane structure, SEM photographs confirm homogeneous morphology and non-failure membranes. It is found that these membranes have good $CO_2$ selectivity. In addition, the membranes are stable in the range of 2 to 10 bar, and by increasing molecular weight of PEG, the pressure does not have a significant effect on permeation, especially at pressures greater than 4 bar. From the observed results, an increase in permeability with increasing the molecular weight of polyethylene glycol is predictable. The PSF/PEG10000 composite membrane with 20-wt% PEG is the most permeable membrane rather than $CO_2$. In addition, the membrane is used to isolate $CO_2/N_2$ separation better than the other composite membranes used in this study. The selectivity of composite membranes, in molecular weights and in different polyethylene glycol contents, is due to the high flexibility of chains and the diffusion of material passing through the membrane as well as the increased solubility due to the interaction with polyether polar heads as another effective factor in the transfer of the studied gases. Tensile strength and Young's modulus results initially led to a reduction in mechanical strength due to incomplete miscibility, but ultimately, with increasing PEG weight, increased tensile strength and Young's modulus because of complete miscibility. DSC test used to check the glass transition temperature. In the low weight percent of PEG, two glass transition temperatures were obtained which indicated incomplete miscibility. However, with increasing PEG weight, a single glass transition temperature was obtained due to complete miscibility. TGA test used to analyze the thermal stability of composite membranes. By adding PEG polymer to a PSF polymer, it reduces thermal stability. However, by increasing the weight percent of PEG, it increased thermal stability.

## References

1. Sridhar S, Smitha B, Ramakrishna M, Aminabhavi TM (2006) Modified poly(phenylene oxide) membranes for the separation of carbon dioxide from methane. J Membr Sci 280:202–209. https://doi.org/10.1016/j.memsci.2006.01.019

2. Mannan HA, Mukhtar H, Murugesan T, Nasir R, Mohshim DF, Mushtaq A (2013) Recent applications of polymer blends in gas separation membranes. Chem Eng Technol 36:1838–1846. https://doi.org/10.1002/ceat.201300342
3. Teodorescu M, Bercea M, Morariu S (2018) Miscibility study on polymer mixtures in dilute solution. Colloids Surf A 559:325–333. https://doi.org/10.1016/j.colsurfa.2018.09.062
4. Roy S, Singha N (2017) Polymeric nanocomposite membranes for next generation pervaporation process: Strategies, challenges and future prospects. Membranes 7:53
5. Darvell BW (2018) Chapter 3 – Polymers. In: Darvell BW (ed) Materials science for dentistry, 10th edn. Woodhead Publishing, Sawston, pp 70–91
6. Robeson LM, Liu Q, Freeman BD, Paul DR (2015) Comparison of transport properties of rubbery and glassy polymers and the relevance to the upper bound relationship. J Membr Sci 476:421–431. https://doi.org/10.1016/j.memsci.2014.11.058
7. Meshkat S, Kaliaguine S, Rodrigue D (2018) Mixed matrix membranes based on amine and non-amine MIL-53(Al) in Pebax® MH-1657 for $CO_2$ separation. Sep Purif Technol 200:177–190. https://doi.org/10.1016/j.seppur.2018.02.038
8. Sethu Lakshmi MB, Francis BS, Kumar A (2018) Chapter 17-Introduction to gas transport through polymer membranes. In: Thomas S, Wilson RS, Kumar A, George SC (eds) Transport properties of polymeric membranes. Elsevier, Amsterdam, pp 349–361
9. Rahman MM, Filiz V, Shishatskiy S, Abetz C, Georgopanos P, Khan M, Neumann S, Abetz V (2015) Influence of poly(ethylene glycol) segment length on $CO_2$ permeation and stability of polyactive membranes and their nanocomposites with PEG POSS. ACSAppl Mat Inter 7:12289–12298
10. Azizi N, Mohammadi T, Behbahani RM (2017) Synthesis of a new nanocomposite membrane (PEBAX-1074/PEG-400/$TiO_2$) in order to separate $CO_2$ from $CH_4$. J Nat Gas Sci Eng 37:39–51
11. Akbarian I, Fakhar A, Ameri E, Sadeghi M (2018) Gas-separation behavior of poly(ether sulfone)–poly(ethylene glycol) blend membranes. J Appl Polym Sci 135:46845. https://doi.org/10.1002/app.46845
12. Li J, Wang S, Nagai K, Nakagawa T, Mau AWH (1998) Effect of polyethyleneglycol (PEG) on gas permeabilities and permselectivities in its cellulose acetate (CA) blend membranes. J Membr Sci 138:143–152. https://doi.org/10.1016/S0376-7388(97)00212-3
13. Mani S, Khare R (2018) Effect of chain flexibility and interlayer interactions on the local dynamics of layered polymer systems. Macromolecules 51:576–588. https://doi.org/10.1021/acs.macromol.7b01519
14. Semsarzadeh MA, Sadeghi M, Barikani M (2008) Effect of chain extender length on gas permeation properties of polyurethane membranes. Iran Polym J 17(6):431–440
15. Semsarzadeh MA, Sadeghi M, Barikani M (2008) Effect of polyol and chain extender length on the gas separation properties of polyurethane. IPJ 17:431–440
16. Alias SS, Harun Z, Shohur MF (2019) Effect of monovalent and divalent ions in non-solvent coagulation bath-induced phase inversion on the characterization of a porous polysulfone membrane. Polym Bull. https://doi.org/10.1007/s00289-019-02689-z
17. Kalantari K, Moradihamedani P, Ibrahim NA, Abdullah AHB, Afifi ABM (2018) Polysulfone mixed-matrix membrane incorporating talc clay particles for gas separation. Polym Bull 75:3723–3738. https://doi.org/10.1007/s00289-017-2234-5
18. Boroglu MS, Gurkaynak MA (2011) Fabrication and characterization of silica modified polyimide–zeolite mixed matrix membranes for gas separation properties. Polym Bull 66:463–478. https://doi.org/10.1007/s00289-010-0286-x
19. Sridhar S, Veerapur RS, Patil MB, Gudasi KB, Aminabhavi TM (2007) Matrimid polyimide membranes for the separation of carbon dioxide from methane. J Appl Polym Sci 106:1585–1594. https://doi.org/10.1002/app.26306
20. Sridhar S, Smitha B, Mayor S, Prathab B, Aminabhavi TM (2007) Gas permeation properties of polyamide membrane prepared by interfacial polymerization. J Mater Sci 42:9392–9401. https://doi.org/10.1007/s10853-007-1813-5
21. Wang Y, Darensbourg DJ (2018) Carbon dioxide-based functional polycarbonates: metal catalyzed copolymerization of $CO_2$ and epoxides. Coord Chem Rev 372:85–100. https://doi.org/10.1016/j.ccr.2018.06.004
22. Motokucho S, Yamada H, Suga Y, Morikawa H, Nakatani H, Urita K, Moriguchi I (2018) Synthesis of an aliphatic hyper-branched polycarbonate and determination of its physical properties for solid polymer electrolyte use. Polymer 145:194–201. https://doi.org/10.1016/j.polymer.2018.05.010

23. Motealleh B, Huang F, Largier TD, Khan W, Cornelius CJ (2019) Solution-blended sulfonated polyphenylene and branched poly(arylene ether sulfone): synthesis, state of water, surface energy, proton transport, and fuel cell performance. Polymer 160:148–161. https://doi.org/10.1016/j.polymer.2018.11.045
24. Largier T, Huang F, Kahn W, Cornelius CJ (2019) Poly(phenylene) synthesized using Diels-Alder chemistry and its sulfonation: sulfonate group complexation with metal counter-ions, physical properties, and gas transport. J Membr Sci 572:320–331. https://doi.org/10.1016/j.memsci.2018.11.024
25. Sridhar S, Suryamurali R, Smitha B, Aminabhavi TM (2007) Development of crosslinked poly(ether-block-amide) membrane for $CO_2/CH_4$ separation. Colloids Surf, A 297:267–274. https://doi.org/10.1016/j.colsurfa.2006.10.054
26. Sridhar S, Aminabhavi TM, Mayor SJ, Ramakrishna M (2007) Permeation of carbon dioxide and methane gases through novel silver-incorporated thin film composite PEBAX membranes. Ind Eng Chem Res 46:8144–8151. https://doi.org/10.1021/ie070114k
27. Sridhar S, Smitha B, Suryamurali R, Aminabhavi TM (2008) Synthesis, characterization and gas permeability of an activated carbon-loaded PEBAX 2533 membrane. Des Monomers Polym 11:17–27. https://doi.org/10.1163/156855508X292392
28. Wang N, Xu P, Wu C, Wu R, Shou D (2019) Preparation of micro-cell membrane chromatographic columns with polyvinyl alcohol-modified polyether ether ketone tube as cellular membrane carrier. J Chromatogr B 1104:102–108. https://doi.org/10.1016/j.jchromb.2018.11.014
29. Mohr JM, Paul DR, Tullos GL, Cassidy PE (1991) Gas transport properties of a series of poly(ether ketone) polymers. Polymer 32:2387–2394. https://doi.org/10.1016/0032-3861(91)90079-X
30. Andrady AL, Llorente MA, Mark JE (1991) Some dynamic mechanical properties of unimodal and bimodal networks of poly(dimethylsiloxane). Polym Bull 26:357–362. https://doi.org/10.1007/BF00587981
31. Ishihara R, Yamaguchi Y, Tanabe K, Makino Y, Nishio K (2019) Preparation of Pt/WO3-coated polydimethylsiloxane membrane for transparent/flexible hydrogen gas sensors. Mater Chem Phys 226:226–229. https://doi.org/10.1016/j.matchemphys.2018.12.052
32. Sridhar S, Aminabhavi TM, Ramakrishna M (2007) Separation of binary mixtures of carbon dioxide and methane through sulfonated polycarbonate membranes. J Appl Polym Sci 105:1749–1756. https://doi.org/10.1002/app.24628
33. Houde AY, Kulkarni SS, Kharul UK, Charati SG, Kulkarni MG (1995) Gas permeation in polyarylates: effects of polarity and intersegmental mobility. J Membr Sci 103:167–174. https://doi.org/10.1016/0376-7388(95)00324-6
34. Patil MB, Patil SA, Veerapur RS, Aminabhavi TM (2007) Novel Poly(vinyl alcohol)-tetraethoxysilane hybrid matrix membranes as oxygen barriers. J Appl Polym Sci 104:273–278. https://doi.org/10.1002/app.25589
35. Kim JH, Ha SY, Nam SY, Rhim JW, Baek KH, Lee YM (2001) Selective permeation of $CO_2$ through pore-filled polyacrylonitrile membrane with poly(ethylene glycol). J Membr Sci 186:97–107. https://doi.org/10.1016/S0376-7388(00)00670-0
36. Chakrabarty B, Ghoshal AK, Purkait MK (2008) SEM analysis and gas permeability test to characterize polysulfone membrane prepared with polyethylene glycol as additive. J Colloid Interface Sci 320:245–253. https://doi.org/10.1016/j.jcis.2008.01.002
37. Sadeghi M, PourafshariChenar M, Rahimian M, Moradi S, Dehaghani AHS (2008) Gas permeation properties of polyvinylchloride/polyethyleneglycol blend membranes. J Appl Polym Sci 110:1093–1098. https://doi.org/10.1002/app.28740
38. Yave W, Car A, Peinemann K-V, Shaikh MQ, Rätzke K, Faupel F (2009) Gas permeability and free volume in poly(amide-b-ethylene oxide)/polyethylene glycol blend membranes. J Membr Sci 339:177–183. https://doi.org/10.1016/j.memsci.2009.04.049
39. Pritchard C (1995) Polymeric gas separation membranes, by R. E. Kesting and A. K. Fritzsche. Wiley Interscience, New York, 1993. Pp. xi + 416, price £49.60, US$68.95. ISBN 0–471–56931–3. Polymer International 36: 102–102. https://doi.org/10.1002/pi.1995.210360116
40. Mars J, Wali M, Delille R, Dammak F (2015) Low velocity impact behavior of glass fibre-reinforced polyamide. In: Multiphysics modelling and simulation for systems design and monitoring. Springer, Cham, pp 469–479
41. Panapitiya N, Wijenayake S, Nguyen D, Karunaweera C, Huang Y, Balkus K, Musselman I, Ferraris J (2016) Compatibilized immiscible polymer blends for gas separations. Materials (Basel, Switzerland) 9:643. https://doi.org/10.3390/ma9080643

42. Ibrahim B, Alghazali K (2010) Influence of polymer blending on mechanical and thermal properties. Mod Appl Sci. https://doi.org/10.5539/mas.v4n9p157
43. Sugimura A, Asai M, Matsunaga T, Akagi Y, Sakai T, Noguchi H, Shibayama M (2013) Mechanical properties of a polymer network of Tetra-PEG gel. Polym J 45:300–306
44. Uemura T, Kaseda T, Sasaki Y, Inukai M, Toriyama T, Takahara A, Jinnai H, Kitagawa S (2015) Mixing of immiscible polymers using nanoporous coordination templates. Nat Commun 6:7473. https://doi.org/10.1038/ncomms8473
45. Runt J Huang J (2002) Polymer blends and copolymers. In: Applications to polymers and plastics, pp 273–294
46. Sanaeepur H, Ebadi Amooghin A, Moghadassi A, Kargari A, Moradi S, Ghanbari D (2012) A novel acrylonitrile–butadiene–styrene/poly(ethylene glycol) membrane: preparation, characterization, and gas permeation study. Polym Adv Technol 23:1207–1218. https://doi.org/10.1002/pat.2031
47. Robeson LM (1999) Polymer membranes for gas separation. Curr Opin Solid State Mat Sci 4:549–552
48. Lin H, Freeman BD (2006) Gas permeation and diffusion in cross-linked poly(ethylene glycol diacrylate). Macromolecules 39:3568–3580. https://doi.org/10.1021/ma051686o
49. Hu X, Tang J, Blasig A, Shen Y, Radosz M (2006) $CO_2$ permeability, diffusivity and solubility in polyethylene glycol-grafted polyionic membranes and their $CO_2$ selectivity relative to methane and nitrogen. J Membr Sci 281:130–138. https://doi.org/10.1016/j.memsci.2006.03.030
50. Han J, Lee W, Choi JM, Patel R, Min B-R (2010) Characterization of polyethersulfone/polyimide blend membranes prepared by a dry/wet phase inversion: precipitation kinetics, morphology and gas separation. J Membr Sci 351:141–148. https://doi.org/10.1016/j.memsci.2010.01.038
51. Bos A, Pünt IGM, Wessling M, Strathmann H (1999) $CO_2$-induced plasticization phenomena in glassy polymers. J Membr Sci 155:67–78. https://doi.org/10.1016/S0376-7388(98)00299-3
52. Lin H, Freeman BD (2004) Gas solubility, diffusivity and permeability in poly(ethylene oxide). J Membr Sci 239:105–117. https://doi.org/10.1016/j.memsci.2003.08.031